Neutron-induced fission cross sections of ^{242}Pu from 0.3 MeV to 3 MeV

P. Salvador-Castiñeira,[1,2,*] T. Bryś,[2] R. Eykens,[2] F.-J. Hambsch,[2,†] A. Göök,[2] A. Moens,[2] S. Oberstedt,[2] G. Sibbens,[2]
D. Vanleeuw,[2] M. Vidali,[2] and C. Pretel[1]

[1]*Institute of Energy Technologies, Technical University of Catalonia, Avda. Diagonal 647, E-08028 Barcelona, Spain*
[2]*European Commission, Joint Research Centre, Institute for Reference Materials and Measurements (JRC-IRMM),
Retieseweg 111, B-2440 Geel, Belgium*

The majority of the next generation of nuclear power plants (GEN-IV) will work in the fast-neutron-energy region, as opposed to present day thermal reactors. This leads to new and more accurate nuclear-data needs for some minor actinides and structural materials. Following those upcoming demands, the Organisation for Economic Cooperation and Development Nuclear Energy Agency performed a sensitivity study. Based on the latter, an improvement in accuracy from the present 20% to 5% is required for the ^{242}Pu(n, f) cross section. Within the same project both the ^{240}Pu(n, f) cross section and the ^{242}Pu(n, f) cross section were measured at the Van de Graaff accelerator of the Joint Research Centre at the Institute for Reference Materials and Measurements, where quasimonoenergetic neutrons were produced in an energy range from 0.3 MeV up to 3 MeV. A twin Frisch-grid ionization chamber has been used in a back-to-back configuration as fission-fragment detector. The ^{242}Pu(n, f) cross section has been normalized to three different isotopes: ^{237}Np(n, f), ^{235}U(n, f), and ^{238}U(n, f). A comprehensive study of the corrections applied to the data and the uncertainties associated is given. The results obtained are in agreement with previous experimental data at the threshold region up to 0.8 MeV. The resonance-like structure at 0.8 to 1.1 MeV, visible in the evaluations and in most previous experimental values, was not reproduced with the same intensity in this experiment. For neutron energies higher than 1.1 MeV, the results of this experiment are slightly lower than the Evaluated Nuclear Data File/B-VII.1 evaluation but in agreement with the experiment of Tovesson *et al.* (2009) as well as Staples and Morley (1998). Finally, for energies above 1.5 MeV, the results show consistency with the present evaluations.

I. INTRODUCTION

For the next generation of nuclear power plants (GEN-IV), four of the six designs currently under study are based on a fast neutron-energy spectrum instead of a thermal one. Consequently, there are upcoming needs for the nuclear-data community to meet more stringent requirements in order to improve the accuracy on the performance of simulations codes in this energy region. To address these aspects, a sensitivity study was performed by the Nuclear Energy Agency (NEA) [1] with the outcome of a list of high priorities of the most important isotopes and their relevant quantities. Not only for isotopes that eventually would be part of the fuel mixture, but also for structural materials intended to surround the reactor core. Within the high-priority list it is requested to improve the accuracy of the neutron-induced fission cross section of ^{242}Pu from the current 20% to a target of 5%.

Several projects worldwide tackled this request with the goal to provide new relevant data. Among them, the Accurate

Nuclear Data and Energy Sustainability Collaboration (AN-DES) [2] aimed to address several data needs for the design of fast reactors and to improve the current knowledge on nuclear data, specifically in the fast-neutron-energy region. The experiment that will be presented in this paper was part of the ANDES collaboration and was performed together with the measurement of the ^{240}Pu(n, f) cross section presented elsewhere [3].

Most of the data sets available in the Experimental Nuclear Reaction Data Library (EXFOR) [4] for the ^{242}Pu(n, f) cross section date from the 1970s and just two of them are from the last decade. Figure 1 presents some of the most relevant experiments in the neutron-energy range where this experiment was focused together with the current evaluations (for clearness not all data points are shown). The spread of the data is very large mainly due to the values of Butler (1960) [5] and Fomushkin and Gutnikova (1970) [6]. Besides that, above 1 MeV two groups of data sets can be distinguished. The first one being the values of Weigmann *et al.* (1984) [7] and the second a subset of the other data sets Bergen and Fullwood (1970) [8], Auchampaugh *et al.* (1971) [9], Meadows (1978) [10], Staples and Morley (1998) [11], and Tovesson *et al.* (2009) [12]). Nevertheless, the two groups are converging at neutron energies above 2.5 MeV. In addition, the spread of the data around the resonance-like structure visible at 1 to 1.1 MeV is quite large; thus, its intensity is not well established. The evaluations available are grouped in two: the Evaluated Nuclear Data File (ENDF/B-VII.1) [13] and the Japanese Evaluated Nuclear Data Library (JENDL 4.0) [14]; and the

---
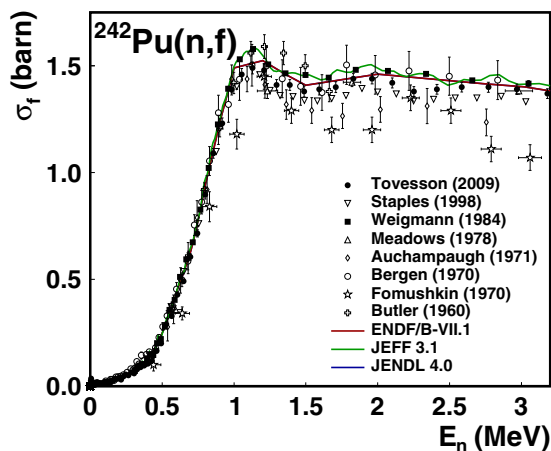
FIG. 1. (Color online) Summary of the most relevant experiments performed on the neutron-induced-fission cross section of ^{242}Pu compared with current evaluations. The evaluations chosen are ENDF/B-VII.1 [13], JEFF 3.1 [15], and JENDL 4.0 [14]. The ENDF/B-VII.1 evaluation follows perfectly the JENDL 4.0. The experimental data sets shown are Butler (1960) [5] (open crosses), Fomushkin and Gutnikova (1970) [6] (open stars), Bergen and Fullwood (1970) [8] (open circles), Auchampaugh *et al.* (1971) [9] (open diamonds), Meadows (1978) [10] (open up triangles), Weigmann *et al.* (1984) [7] (full squares), Staples and Morley (1998) [11] (open down triangles), and Tovesson *et al.* (2009) [12] (full circles). Selected data are shown for visibility of the plot. Data found as a ratio of ^{235}U were normalized to the ENDF/B-VII.1 evaluation of this isotope. Further explanation is given in the text.

Joint Evaluated Fission and Fusion File (JEFF 3.1) [15]. Actually, the ENDF/B-VII.1 evaluation follows exactly the JENDL 4.0 evaluation, which used most of the data sets presented. In contrast, the JEFF 3.1 evaluation follows the experimental data of Weigmann *et al.* (1984). The uncertainties presented in these data sets are often not explained in detail and, most of the time, the total uncertainty does not include the uncertainty of the reference cross section used.

To improve the knowledge of the ^{242}Pu(n, f) cross section it was decided to use three different reference isotopes. As primary standard ^{235}U(n, f), ^{238}U(n, f) as secondary standard, and ^{237}Np(n, f). Additionally, ^{237}Np(n, f) and ^{238}U(n, f) were benchmarked by using ^{235}U(n, f). An extended explanation is given below.

II. EXPERIMENT SETUP

A. Van de Graaff accelerator

The neutrons were generated through (p,n) reactions at the Van de Graaff accelerator (VdG) of the Joint Research Centre at the Institute for Reference Materials and Measurements (JRC-IRMM). A quasimonoenergetic neutron flux was produced from neutron energies of 0.3 MeV up to 1.8 MeV by using the ^{7}Li$(p,n)^7$Be reaction; and from 1.6 MeV up to 3.0 MeV by using the T$(p,n)^3$He reaction. The neutron-producing targets were water cooled by using a water-layer thickness of 1 to 3 mm. The Monte Carlo code MCNP [16] was
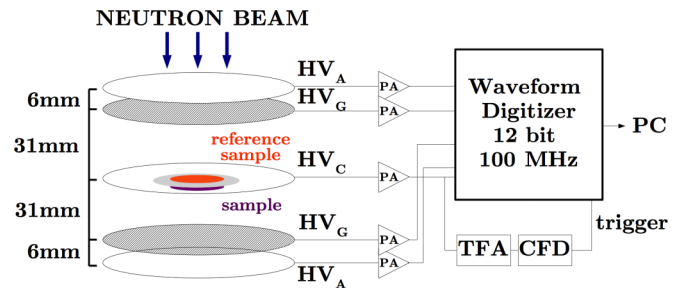
FIG. 2. (Color online) Scheme of the twin Frisch-grid ionization chamber with two samples in a back-to-back configuration followed by the digital electronics used for this experiment.

used in order to study the influence of the water cooling system on the degradation of the neutron energy (discussed below).

B. Fission-fragment detector

The fission fragments (FFs) produced were detected by using a twin Frisch-grid ionization chamber (TFGIC). A detailed description of the detector used in the present experiment is given in Ref. [3]. A schematic view of the setup can be seen in Fig. 2, where the TFGIC is plotted together with the associated electronic scheme. The cathode-grid distance was chosen in order to fully stop the FFs before reaching the grid. For cross-section experiments a common choice is to place both samples in the cathode holder, the sample under study and the reference sample, in a back-to-back geometry; in this way, a measurement of the neutron flux in the exact place, where the samples are, can be avoided.

C. Data acquisition

A 12 bit, 100 MHz waveform digitizer (WFD) was employed to store the preamplifier raw signals of the charges collected by the electrodes. The trigger of all the WFD cards was made from the cathode preamplifier signal after treatment with a timing filter amplifier (TFA) and a constant fraction discriminator (CFD). To avoid triggering the whole system with α-particle signals coming, especially, from the ^{242}Pu sample, an electronic threshold was set in the CFD. The storage of the signals was done with a data-acquisition system (DAQ) built in C++ using ROOT as framework [17,18] and which was developed at JRC-IRMM.

D. Signal processing

The signals were analyzed offline via a digital signal processing (DSP) code developed at JRC-IRMM. A baseline correction and a CR-RC^4 filter were applied to the signals to obtain their pulse height (PH). The PH distributions were corrected later for the grid inefficiency [19].

E. Sample description

An overview of the sample properties is given in Table I, complementing the description given in Ref. [3]. As mentioned in Ref. [3], all the samples were produced by the target-preparation group at JRC-IRMM.

TABLE I. Description of the ^{242}Pu sample and the reference samples used (^{237}Np, ^{238}U, and ^{235}U) [20–22].

	^{242}Pu	^{237}Np	^{235}U	^{238}U
Method	Electrodeposition	Vacuum deposition	Vacuum deposition	Vacuum deposition
Mass[a] (μg)	671 (0.9%)	390 (0.3%)	584 (2%)	577 (0.4%)
Diameter (mm)	30 (0.1%)	12.7	28	30
Areal density (μg/cm^2)	95.3 (0.8%)	308 (0.3%)	94.8 (2%)	81.7 (0.4%)
Backing	Aluminum	Stainless steel	Stainless steel	Transparent
α activity (MBq)	0.0984 (0.3%)	0.001 (0.1%)	265.7 Bq[b] (2%)	7 Bq (0.5%)
%^{238}Pu	0.0027	99.8% ^{237}Np	99.5% ^{235}U	99.99% ^{238}U
%^{239}Pu	0.0044	0.2% ^{238}Pu	0.2% ^{234}U	<0.02% ^{234}U
%^{240}Pu	0.0192		0.03% ^{236}U	
%^{241}Pu	0.0081		0.3% ^{238}U	
%^{242}Pu	99.9652			
%^{244}Pu	0.0004			

[a]The sample mass corresponds just to the main isotope and not to the total mass of the chemical compound.
[b]The sample activity of the ^{235}U sample considers the contribution of the ^{234}U and ^{235}U isotopes.

By using fluorescence images, the homogeneity of the samples produced via electrodeposition and via vacuum deposition was evaluated. The vacuum-deposited samples, specifically the ^{237}Np, presented a uniform distribution of α activity on their surfaces. The inhomogeneities visible in the electrodeposited sample (i.e., ^{242}Pu) were quantified by a low-solid-angle α-particle-counting measurement. The inhomogeneities in the outer layer of the ^{242}Pu sample were quantified to be 7.4% larger with respect to the inner one.

F. Shielding

Pictures of the experimental setup with and without shielding were presented in Ref. [3]. The setup with the shielding was employed only when the measurements were done relative to ^{235}U(n, f). The main purpose of shielding the TFGIC with a paraffin-B$_4$C layer was to avoid neutrons, scattered in the target hall, interacting with the ^{235}U sample at a much lower energy than the nominal beam energy. The impact of low-energy neutrons must be minimized when measuring again a fissile isotope standard, because of the much larger neutron-induced cross section at those energies.

III. CROSS-SECTION MEASUREMENT

In the present case the ratios measured were ^{242}Pu $(n, f)/^{237}$Np(n, f), ^{242}Pu$(n, f)/^{238}$U(n, f), and ^{242}Pu$(n, f)/$ ^{235}U(n, f). The ratio ^{242}Pu$(n, f)/^{238}$U(n, f) was renormalized by using the measured ratio ^{238}U$(n, f)/^{235}$U(n, f), as explained in Ref. [3].

The corrections applied to the measured data were loss of fission events due to the electronic threshold; counts due to spontaneous fission; self-absorption and geometrical efficiency; neutron spectrum, sample inhomogeneity and solid angle; corrections due to the excited state of the ^{7}Li$(p,n)^7$Be reaction; and corrections due to the down-scattered neutrons. In the following only corrections that are significantly different compared to those discussed in Ref. [3] will be explained.

To start with, the spontaneous fission rate of the ^{242}Pu was about 0.5 fissions/s. Therefore, this decay will compete with the neutron-induced fission over the whole neutron-energy range considered here, but will be most important close to and below the fission threshold ($E_n < 0.8$ MeV). Special attention had been given to redetermine the spontaneous fission half-life of this isotope, i.e., $T_{1/2,SF} = 6.74 \times 10^{10}$ y (1.3%) [23].

The neutron background was studied by means of MCNP [16] simulations for both setups. The main contribution to the neutron-energy loss was due to the water cooling system of the neutron-producing target. This energy loss meant that at the sample deposits the neutron energy spectrum was no longer quasimonoenergetic, but the range of energy was broader. In the specific case of using the ^{235}U reference sample, an increase of the reference sample fission count rate will be produced, because the ^{235}U(n, f) cross section increases when the neutron energy decreases. Therefore, the calculated (n, f) cross section of the isotope of interest would be underestimated. The correction factors were calculated as the ratio of the flux at the neutron energy of interest folded with the (n, f) cross section of the sample isotope considered $[\Phi(E_n)\sigma(E_n)]$ and the flux as a function of the neutron energy impinging on the sample deposits folded with the neutron-induced fission cross section of the isotope of interest $[\sum_i \Phi(E_i)\sigma(E_i)]$. In Fig. 3 the correction factors for *setup #1* (no shielding around the TFGIC) are presented.

A. Sources of uncertainty

All uncertainties related to this experiment are summarized in Table II. The highest contribution comes from the spontaneous fission counts [23], the uncertainty on the ^{235}U mass, the geometrical efficiency uncertainty and, finally, the uncertainty associated with the ^{237}Np(n, f) normalization.

B. Results

The absolute values measured for the three ratios ^{242}Pu$(n, f)/^{237}$Np(n, f) (blue triangles), ^{242}Pu$(n, f)/^{238}$U (n, f) [red dots; renormalized by using ^{238}U$(n, f)/^{235}$U(n, f)], and ^{242}Pu$(n, f)/^{235}$U(n, f) (green stars) are plotted in Fig. 4.

First, the data taken relative to the ^{237}Np(n, f) cross section (blue triangles) can reproduce the fission threshold below 0.7 MeV. From this energy onwards the difference with
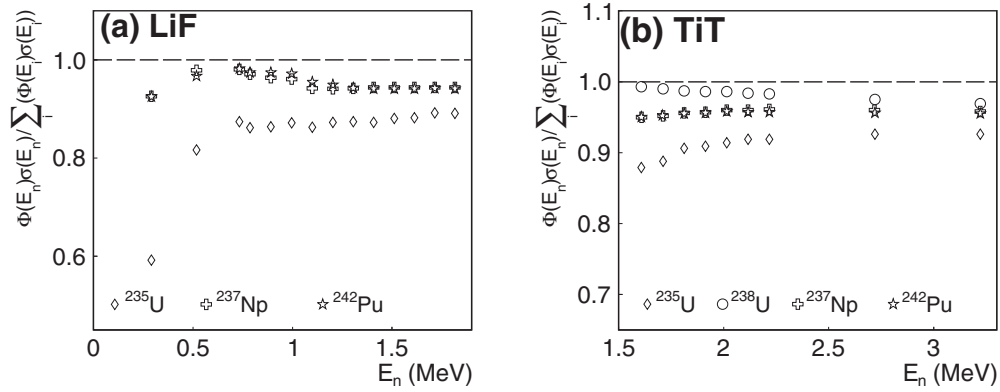
FIG. 3. Correction factors to account for the neutrons outside the region of interest produced by a thermalization in *setup #1* between the neutron-producing target and the fissile deposits. The results given are the ratio of the flux at the neutron energy of interest folded with the (n, f) cross section of the sample isotope considered $[\Phi(E_n)\sigma(E_n)]$ and the flux as function of the neutron energy impinging on the sample deposits folded with the neutron-induced fission cross section of the isotope of interest $[\sum_i \Phi(E_i)\sigma(E_i)]$. (a) Using a LiF neutron-producing target. (b) Using a TiT neutron-producing target. For each case the initial neutron energy was a distribution as a function of the emission angle. The tables were taken from Refs. [24,25].

theENDF/B-VII.1 evaluation increases to 10% at neutron energies between 1.3 and 1.5 MeV. Our data cannot reproduce the resonance-like structure around 1.1 MeV or, at least, it is much less pronounced. Between 1.5 MeV and 1.8 MeV, our data are around 5% to 6% lower than all evaluations.

Second, the ^{242}Pu(n, f) cross-section data obtained from the ratio ^{242}Pu$(n, f)/^{238}$U(n, f) after renormalizing them with a ratio measurement of ^{238}U$(n, f)/^{235}$U(n, f) and the ^{235}U(n, f) ENDF/B-VII.1 evaluation (red dots) are lower than the present evaluations for neutron energies below 2.5 MeV yet in agreement with the values obtained relative to the ^{237}Np(n, f). Above 2.5 MeV, our results agree with the evaluated data files.

Third, the green stars present the absolute ^{242}Pu(n, f) data taken as a ratio with ^{235}U(n, f) by using two different neutron-producing targets ^{7}Li$(p,n)^7$Be (0.3 MeV up to 1.8 MeV) and T$(p,n)^3$He (1.6 MeV up to 3.0 MeV). The results, when using the LiF target, are in good agreement with the results obtained by using the ^{237}Np(n, f) as reference. At 1.8 MeV, the neutron energy common for measurements done with the LiF target

and the TiT target, a 5% difference in the result is observed; this effect is currently under investigation. The data obtained when using the TiT is consistent with the present evaluations.

A weighted average was calculated for all subsets of data; the results are shown in Fig. 5 together with previous experimental data and most recent evaluations. The neutron-energy window chosen for each weighted data point was the wider window from the individual data points to be weighted.
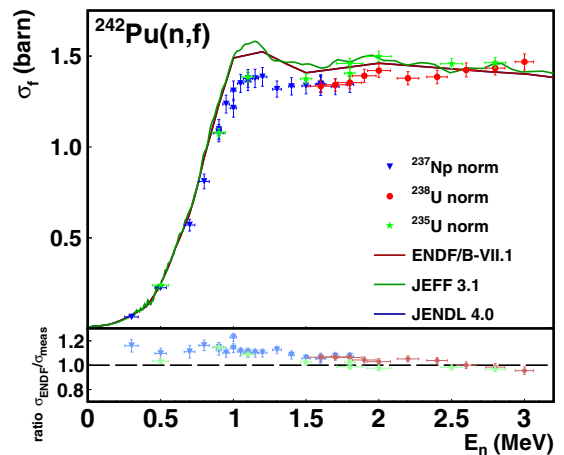
FIG. 4. (Color online) Neutron-induced fission cross section of ^{242}Pu using as reference ^{237}Np(n, f) (blue triangles), ^{235}U(n, f) (green stars), and ^{238}U(n, f) (red dots). At the fission threshold the ^{237}Np data set and the ^{235}U data set are in agreement. At the overlapping region where the two (p,n) reactions can be used the values of the ^{237}Np and ^{238}U data sets coincide. A 5% difference is visible when measuring the same ^{242}Pu$(n, f)/^{235}$U(n, f) ratio by using the Li reaction or the TiT reaction. The discrepancy between this experiment and the present evaluations around 1 MeV is 10%. At the plateau region, this experiment is up to 5% lower than the evaluated data files in the case of the measurements relative to ^{237}Np(n, f) and ^{238}U(n, f). When using the ^{235}U(n, f) cross section for normalization and the TiT reaction, the values obtained are the ones predicted by the evaluations.

TABLE II. Summary of the systematic uncertainties associated with the cross-section measurements.

Uncertainty source	
Statistical	0.5%
Counts SF	<1.3%
^{242}Pu mass	0.9%
^{237}Np mass	0.3%
^{235}U mass	1.5%-2%
^{238}U mass	0.5%
Efficiency	1%
Sample purity	0.001%
Correction of neutron spectrum	<0.2%
MCNP correction of thermalized flux (ratio)	0.5%
^{237}Np ENDF evaluation	2.2% to 4%
^{238}U standard [26]	0.7%
^{235}U standard [26]	<0.8%
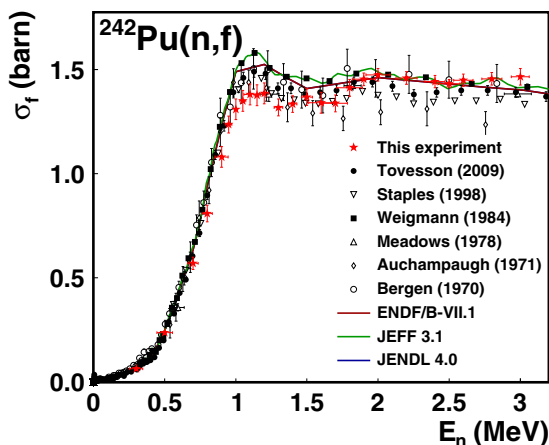
FIG. 5. (Color online) Summary of the results of this experiment (red stars) compared with the most relevant experiments performed on the neutron-induced fission cross section of ^{242}Pu and with current evaluations. The evaluations chosen are ENDF/B-VII.1 [13], JEFF 3.1 [15], and JENDL 4.0 [14]. The JENDL 4.0 evaluation follows perfectly the ENDF/B-VII.1. The experimental data shown are Bergen and Fullwood (1970) [8] (open circles), Auchampaugh *et al.* (1971) [9] (open diamonds), Meadows (1978) [10] (open up triangles), Weigmann *et al.* (1984) [7] (full squares), Staples and Morley (1998) [11] (open down triangles), and Tovesson *et al.* (2009) [12] (full circles). Selected data are shown for legibility of the plot. Data found as a ratio to ^{235}U(n,f) were normalized to the ENDF/B-VII.1 evaluation of this isotope. Further explanation is given in the text.

The uncertainty presented is the larger of the individual data points used to calculate the weighted average. At the fission threshold, the values of this experiment are in agreement with previous experimental data sets available in EXFOR, as well as with the current evaluations. From 0.8 MeV up to 1.5 MeV, our results are systematically lower than the

evaluations; also, the resonance-like structure show a much lower amplitude. Nevertheless, between 1.2 and 1.5 MeV, our data is in agreement with the data of Tovesson *et al.* (2009) [12] and Staples and Morley (1998) [11]. Above 1.5 MeV, the weighted average converges with the present evaluations.

IV. CONCLUSIONS

The neutron-induced fission cross section of ^{242}Pu has been measured in the neutron-energy range from 0.3 MeV up to 3 MeV, following the requests based on the High-Priority Request List of the OECD-NEA. The neutrons were produced via two proton-induced reactions; namely, ^{7}Li$(p,n)^{7}$Be and T$(p,n)^{3}$He, at the Van de Graaff accelerator at JRC-IRMM. A twin Frisch-grid ionization chamber was used as fission fragment detector. This experiment was performed together with the experiment presented in Ref. [3]. The results obtained for the ^{242}Pu(n,f) cross section are in agreement with previous data sets at the fission threshold, without being able to reproduce the resonance-like structure taken up in the evaluated data files and some data sets at 1 to 1.1 MeV. This result cannot be attributed to the finite width of our incident neutron energy bins. Besides the 1 to 1.1 MeV region, at the plateau region this experiment converges with the values obtained by Tovesson *et al.* (2009) and Staples and Morley (1998) and, at neutron energies above 1.5 MeV with the evaluations. The uncertainty budget reached is mainly due to the mass uncertainty of the samples used, the efficiency calculation, and the normalization with the reference cross sections. Yet, the uncertainty associated with each individual data point is always smaller than 5%.

[1] M. Salvatores, *Uncertainty and Target Accuracy Assessment for Innovative Systems Using Recent Covariance Data Evaluations (NEA/WPEC-26)* [Nuclear Energy Agency (OECD), Paris, 2008].

[2] ANDES project, http://www.andes-nd.eu.

[3] P. Salvador-Castiñeira, T. Bryś, R. Eykens, F.-J. Hambsch, A. Göök, A. Moens, S. Oberstedt, G. Sibbens, D. Vanleeuw, M. Vidali, and C. Pretel, Phys. Rev. C **92**, 014620 (2015).

[4] Experimental Nuclear Reaction Data (EXFOR), http://www.nndc.bnl.gov/exfor/exfor.htm.

[5] D. K. Butler, Phys. Rev. **117**, 1305 (1960).

[6] E. Fomushkin and E. Gutnikova, Sov J. Nucl. Phys. **10**, 529 (1970).

[7] H. Weigmann, J. Wartena, and C. Bürkholz, Nucl. Phys. A **438**, 333 (1985).

[8] D. Bergen and R. Fullwood, Nucl. Phys. A **163**, 577 (1971).

[9] G. Auchampaugh, J. Farrell, and D. Bergen, Nucl. Phys. A **171**, 31 (1971).

[10] J. Meadows, Nucl. Sci. Eng. **68**, 360 (1978).

[11] P. Staples and K. Morley, Nucl. Sci. Eng. **129**, 149 (1998).

[12] F. Tovesson, T. S. Hill, M. Mocko, J. D. Baker, and C. A. McGrath, Phys. Rev. C **79**, 014613 (2009).

[13] M. B. Chadwick, M. Herman, P. Obložinský, M. E. Dunn, Y. Danon, A. C. Kahler, D. L. Smith, B. Pritychenko, G. Arbanas, R. Arcilla *et al.*, Nucl. Data Sheets **112**, 2887 (2011).

[14] K. Shibata, O. Iwamoto, T. Nakagawa, N. Iwamoto, A. Ichihara, S. Kunieda, S. Chiba, K. Furutaka, N. Otuka, T. Ohasawa *et al.*, J. Nucl. Sci. Technol. (Abingdon, U.K.) **48**, 1 (2011).

[15] A. Santamarina, D. Bernard, P. Blaise, M. Coste, A. Courcelle, T. Huynh, C. Jouanne, P. Leconte, O. Litaize, S. Mengelle *et al.*, JEFF Report **22**, 2 (2009).

[16] MCNP, https://mcnp.lanl.gov/.

[17] C++, http://www.cplusplus.com/.

[18] ROOT, http://root.cern.ch/drupal/.

[19] A. Göök, F.-J. Hambsch, A. Oberstedt, and S. Oberstedt, Nucl. Instrum. Methods Phys. Res., Sect. A **664**, 289 (2012).

[20] G. Sibbens, A. Moens, R. Eykens, D. Vanleeuw, F. Kehoe, H. Kühn, R. Wynants, J. Heyse, A. Plompen, R. Jakopiĉ, S. Richter, and Y. Aregbe, J. Rad. Nucl. Chem. **299**, 1093 (2014).

[21] S. Pommé (private communication).

[22] A. Göök (private communication).

[23] P. Salvador-Castiñeira, T. Bryś, R. Eykens, F.-J. Hambsch, A. Moens, S. Oberstedt, G. Sibbens, D. Vanleeuw, M. Vidali, and C. Pretel, Phys. Rev. C **88**, 064611 (2013).

[24] H. Liskien and A. Paulsen, At. Data Nucl. Data Tables **11**, 569 (1973).

[25] H. Liskien and A. Paulsen, At. Data Nucl. Data Tables **15**, 57 (1975).

[26] A. D. Carlson, V. G. Pronyaev, D. L. Smith, N. M. Larson, Z. Chen, G. M. Hale, F.-J. Hambsch, E. V. Gai, S.-Y. Oh, S. A. Badikov *et al.*, Nucl. Data Sheets **110**, 3215 (2009).